

Large-scale Augmented Granger Causality (lsAGC) for Connectivity Analysis in Complex Systems: From Computer Simulations to Functional MRI (fMRI)

Axel Wismüller,^{a,b,c,d} and M. Ali Vosoughi^a

^aDepartment of Electrical and Computer Engineering, University of Rochester, NY, USA

^b Department of Imaging Sciences, University of Rochester, NY, USA

^cDepartment of Biomedical Engineering, University of Rochester, NY, USA

^dFaculty of Medicine and Institute of Clinical Radiology, Ludwig Maximilian University, Munich, Germany

ABSTRACT

We introduce large-scale Augmented Granger Causality (lsAGC) as a method for connectivity analysis in complex systems. The lsAGC algorithm combines dimension reduction with source time-series augmentation and uses predictive time-series modeling for estimating directed causal relationships among time-series. This method is a multivariate approach, since it is capable of identifying the influence of each time-series on any other time-series in the presence of all other time-series of the underlying dynamic system. We quantitatively evaluate the performance of lsAGC on synthetic directional time-series networks with known ground truth. As a reference method, we compare our results with cross-correlation, which is typically used as a standard measure of connectivity in the functional MRI (fMRI) literature. Using extensive simulations for a wide range of time-series lengths and two different signal-to-noise ratios of 5 and 15 dB, lsAGC consistently outperforms cross-correlation at accurately detecting network connections, using Receiver Operator Characteristic Curve (ROC) analysis, across all tested time-series lengths and noise levels. In addition, as an outlook to possible clinical application, we perform a preliminary qualitative analysis of connectivity matrices for fMRI data of Autism Spectrum Disorder (ASD) patients and typical controls, using a subset of 59 subjects of the Autism Brain Imaging Data Exchange II (ABIDE II) data repository. Our results suggest that lsAGC, by extracting sparse connectivity matrices, may be useful for network analysis in complex systems, and may be applicable to clinical fMRI analysis in future research, such as targeting disease-related classification or regression tasks on clinical data.

Further author information: (Send correspondence to Ali Vosoughi)

Ali Vosoughi: E-mail: mvosough@ur.rochester.edu

Keywords: machine learning, resting-state fMRI, large-scale Augmented Granger Causality, functional connectivity, autism spectrum disorder

1. INTRODUCTION

Currently, the quantification of directed information transfer between interacting brain areas is one of the most challenging methodological problems in computational neuroscience. A fundamental problem is identifying connectivity in very high-dimensional systems. A common practice has been to transform a high-dimensional system into a simplified representation, e.g. by clustering, Principal, or Independent Component Analysis. The drawback of such methodology is that an identified interaction between such simplified components cannot readily be transferred back into the original high-dimensional space. Thus, directed interactions between the original network nodes can no longer be revealed. Although this significantly limits the interpretation of brain network activities in physiological and disease states, surprisingly little effort has been devoted to circumvent the inevitable information loss induced by the aforementioned frequently employed techniques.

Various methods have been proposed to obtain directional relationships in multivariate time-series data, e.g., transfer entropy [1] and mutual information [2]. However, as the multivariate problem's dimensions increase, computation of the density function becomes computationally expensive [3, 4]. Under the Gaussian assumption, transfer entropy is equivalent to Granger causality [5]. However, the computation of multivariate Granger causality for short time series in large-scale problems is challenging [6, 7]. To address these problems, we have previously proposed a method for multivariate Granger causality analysis using linear multivariate auto-regressive (MVAR) modeling, which simultaneously circumvents the drawbacks of above mentioned simplification strategies by introducing an invertible dimension reduction followed by a back-projection of prediction residuals into the original data space (large-scale Granger Causality, lsGC) [8]. We have also demonstrated the applicability of this approach to resting-state fMRI analysis [9]. Recently, we have also presented an alternative multivariate Granger causality analysis method, large-scale Extended Granger Causality (lsXGC), that uses an augmented dimension-reduced time-series representation for predicting target time-series in the original high-dimensional system directly, i.e., without inverting the dimensionality reduction step [10].

In this paper, we introduce a hybrid of both methods, large-scale Augmented Granger Causality (lsAGC) that combines both invertible dimension reduction and time-series augmentation. It first uses an augmented dimension-reduced time-series representation for prediction in the low-dimensional space, followed by an inversion of the initial dimension reduction step. In the following, we explain the lsAGC algorithm and present quantitative results on synthetic time-series data with known connectivity ground truth. Finally, as an outlook to possible clinical application, we perform a preliminary qualitative analysis of connectivity matrices for fMRI data of

Autism Spectrum Disorder (ASD) patients and typical controls, using a subset of the Autism Brain Imaging Data Exchange II (ABIDE II) data repository.

This work is embedded in our group’s endeavor to expedite artificial intelligence in biomedical imaging by means of advanced pattern recognition and machine learning methods for computational radiology and radiomics, e.g., [11–68].

2. DATA

2.1 Synthetic Networks with Known Ground Truth for Quantitative Analysis

We quantitatively evaluate the performance of lsAGC for network structure recovery using synthetic networks with known ground truth. We constructed ground truth networks with $N = 50$ nodes, each containing 5 modules of 10 nodes with high (low) probability for the existence of directed intra- (inter-) module connections. We simulated two values of additive white Gaussian noise, with signal-to-noise ratios (SNR) of 15 dB and 5 dB, and repeated the experiment 100 times with different noise seed. Networks were realized as noisy stationary multivariate auto-regressive (MVAR) processes of model order $p = 2$ in each of $T = 1000$ temporal process iterations. The network structure was adapted from [69] and [56].

2.2 Functional MRI Data for Qualitative Analysis

The following explanation of participants and data in this section follows the description in [70]: The Autism Brain Imaging Data Exchange II (ABIDE II) initiative has made publicly available MRI data from multiple sites. We used resting-state fMRI data from 59 participants of the online ABIDE II repository (<http://fcon.1000.projects.nitrc.org/indi/abide>) in this analysis, namely the data from the Olin Neuropsychiatry Research Center, Institute of Living at Hartford Hospital [71].

This data set consists of 24 ASD subjects (18-31 years) and 35 typical controls (18-31 years). Autism diagnosis was based on the ASD cutoff of the Autism Diagnostic Observation Schedule-Generic (ADOS-G). The typical controls (TC) were screened for autism using the ADOS-G and any psychiatric disorder based on the Structured Clinical Interview for DSM-IV Axis I Disorders-Research Version (SCID-I RV) [71].

In this data set, resting-state fMRI scans were obtained from all subjects using Siemens Magnetom Skyra Syngo MR D13. The study protocol included: (i) High-resolution structural imaging using T1-weighted magnetization-prepared rapid gradient-echo (MPRAGE) sequence, $TE = 2.88$ ms, $TR = 2200$ ms, isotropic voxel size 1 mm, flip angle 13° . (ii) Resting-state fMRI scans with $TE = 30$ ms, $TR = 475$ ms, flip angle 60° , isotropic voxel size of 3 mm. The acquisition lasted 7 minutes and 37 seconds.

The fMRI data used in this study were pre-processed using standard methodology. Motion correction, brain extraction, and correction for slice timing acquisition were performed. Additional nuisance regression for removing variations due to head motion and physiological processes was carried out. Each data set was finally registered to the 2 mm MNI standard space using a 12-parameter affine transformation. The functional data used in this study was pre-processed using the CONN toolbox (www.nitrc.org/projects/conn) [72]. Additionally, the time-series were normalized to zero mean and unit standard deviation to focus on signal dynamics rather than amplitude [73]. Finally, the brain was parcellated into 90 regions as defined by the Automated Anatomic Labelling (AAL) template [74]. Each regional time-series was represented by the average time-series of all voxels included in the region.

3. ALGORITHM

Large-scale Augmented Granger Causality (lsAGC) has been developed based on 1) the principle of original Granger causality, which quantifies the causal influence of time-series \mathbf{x}_s on time-series \mathbf{x}_t by quantifying the amount of improvement in the prediction of \mathbf{x}_t in presence of \mathbf{x}_s . 2) the idea of dimension reduction, which resolves the problem of the tackling a under-determined system, which is frequently faced in fMRI analysis, since the number of acquired temporal samples usually is not sufficient for estimating the model parameters.⁹

Consider the ensemble of time-series $\mathcal{X} \in \mathbb{R}^{N \times T}$, where N is the number of time-series (Regions Of Interest – ROIs) and T the number of temporal samples. Let $\mathcal{X} = (\mathbf{x}_1, \mathbf{x}_2, \dots, \mathbf{x}_N)^\top$ be the whole multidimensional system and $x_i \in \mathbb{R}^{1 \times T}$ a single time-series with $i = 1, 2, \dots, N$, where $\mathbf{x}_i = (x_i(1), x_i(2), \dots, x_i(T))$. In order to overcome the under-determined problem, first \mathcal{X} will be decomposed into its first p high-variance principal components $\mathcal{Z} \in \mathbb{R}^{p \times T}$ using Principal Component Analysis (PCA), i.e.,

$$\mathcal{Z} = W\mathcal{X}, \quad (1)$$

where $W \in \mathbb{R}^{p \times N}$ represents the PCA coefficient matrix. Subsequently, the dimension-reduced time-series ensemble \mathcal{Z} is augmented by one original time-series \mathbf{x}_s yielding a dimension-reduced augmented time-series ensemble $\mathcal{Y} \in \mathbb{R}^{(p+1) \times T}$ for estimating the influence of \mathbf{x}_s on all other time-series.

Following this, we locally predict the dimension-reduced representation \mathcal{Z} of the original high-dimensional system \mathcal{X} at each time sample t , i.e. $\mathcal{Z}(t) \in \mathbb{R}^{p \times 1}$ by calculating an estimate $\hat{\mathcal{Z}}_{\mathbf{x}_s}(t)$. To this end, we fit an affine model based on a vector of m vector of m time samples of $\mathcal{Y}(\tau) \in \mathbb{R}^{(p+1) \times 1} (\tau = t-1, t-2, \dots, t-m)$, which is $\mathbf{y}(t) \in \mathbb{R}^{m \cdot (p+1) \times 1}$, and a parameter matrix $\mathcal{A} \in \mathbb{R}^{p \times m \cdot (p+1)}$ and a constant bias vector $\mathbf{b} \in \mathbb{R}^{p \times 1}$,

$$\hat{\mathcal{Z}}_{\mathbf{x}_s}(t) = \mathcal{A}\mathbf{y}(t) + \mathbf{b}, \quad t = m+1, m+2, \dots, T. \quad (2)$$

Subsequently, we use the prediction $\hat{\mathcal{Z}}_{\mathbf{x}_s}(t)$ to calculate an estimate of \mathcal{X} at time t , i.e. $\mathcal{X}(t) \in \mathbb{R}^{N \times 1}$ by inverting the PCA of equation (2), i.e.

$$\mathcal{X} = W^\dagger \mathcal{Z}, \quad (3)$$

where $W^\dagger \in \mathbb{R}^{N \times p}$ represents the inverse of the PCA coefficient matrix W , which is calculated as the *Moore–Penrose* pseudoinverse of W .

Now $\hat{\mathcal{X}}_{\setminus \mathbf{x}_s}(t)$, which is the prediction of $\mathcal{X}(t)$ without the information of \mathbf{x}_s , will be estimated. The estimation processes is identical to the previous one, with the only difference being that we have to remove the augmented time-series \mathbf{x}_s and its corresponding column in the PCA coefficient matrix W .

The computation of a lsAGC index is based on comparing the variance of the prediction errors obtained with and without consideration of \mathbf{x}_s . The lsAGC index $f_{\mathbf{x}_s \rightarrow \mathbf{x}_t}$, which indicates the influence of \mathbf{x}_s on \mathbf{x}_t , can be calculated by the following equation:

$$f_{\mathbf{x}_s \rightarrow \mathbf{x}_t} = \log \frac{\text{var}(e_s)}{\text{var}(e_{\setminus s})}, \quad (4)$$

where $e_{\setminus s}$ is the error in predicting \mathbf{x}_t when \mathbf{x}_s was not considered, and e_s is the error, when \mathbf{x}_s was used. Based on preliminary analyses, in this study, we set $p = 7$ and $m = 3$.

4. RESULTS

Quantitative Analysis of Synthetic Networks with Known Ground Truth: Network reconstruction results for the synthetic networks with known ground truth, using the Area Under the Curve (AUC) for Receiver Operating Characteristic (ROC) analysis, are shown in Fig. 1. For each time-series length and each noise level, we performed 100 simulations. As can be seen from Fig. 1, lsAGC consistently outperforms cross-correlation in its ability to accurately recover network structure over a wide range of time-series-lengths in both high- and low-noise scenarios, with a mean AUC for lsAGC for a time-series length of 1000 temporal samples equal to 98.9% and 97.1% for signal-to-noise values of 15 and 5 dB, respectively. On the other hand, cross-correlation performs quite poorly compared to lsAGC with its mean AUC ranging around 0.5 for all examined time-series lengths and noise levels, equivalent to the quality of randomly guessing the presence or absence of network connections.

Qualitative Analysis of Connectivity Matrices Extracted from fMRI Data: Averaged connectivity matrices, which were extracted using lsAGC and cross-correlation, are shown in Fig. 2 for both healthy controls and ASD patients. These matrices were obtained by calculating and then averaging over the connectivity matrices of the 24 ASD patients and 35 typical controls, using the proposed lsAGC algorithm as well as conventional cross-correlation analysis. Visual inspection of the mean connectivity matrices in Fig. 2 reveals subtle differences between ASD patients and healthy controls for both methods, which may be exploited for classification among

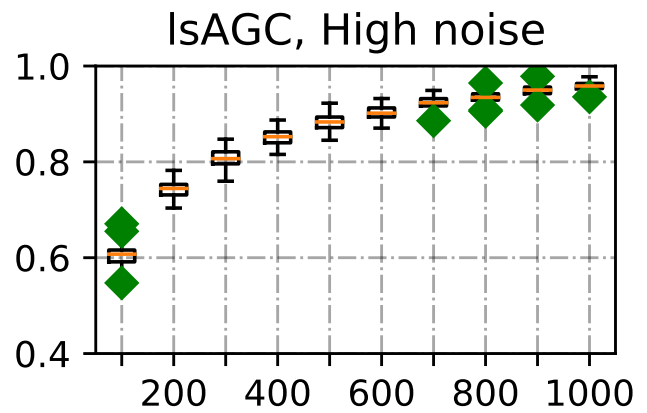
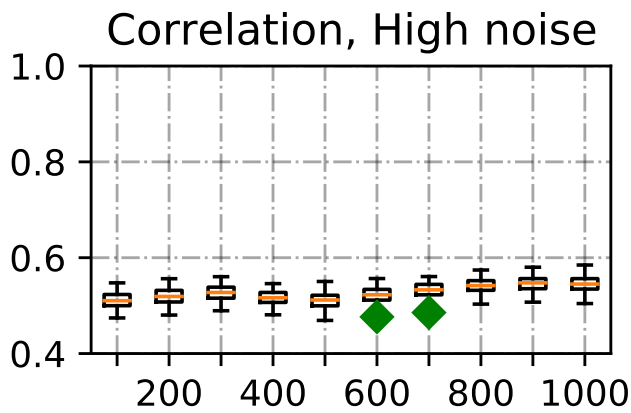
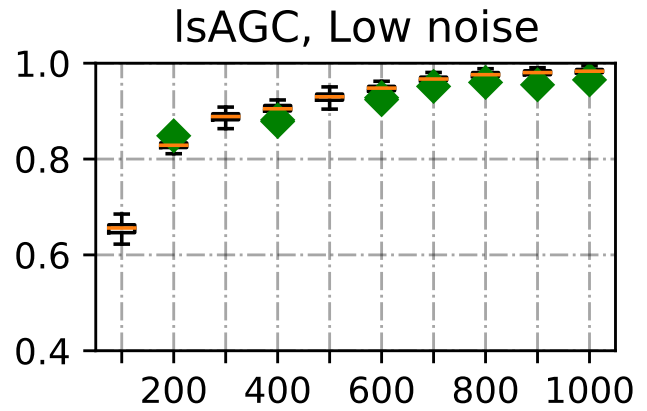
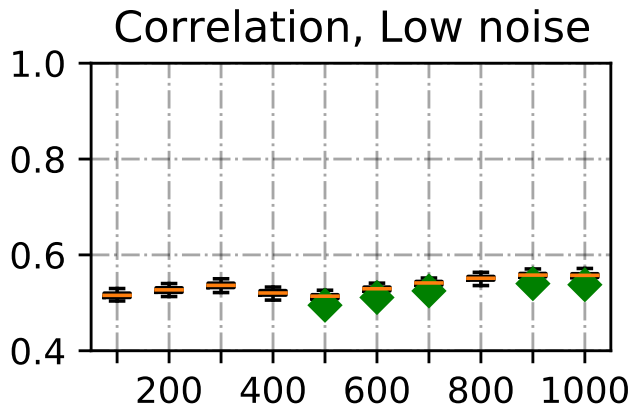


Figure 1. Quantitative performance comparison of cross-correlation and lsAGC for recovery of synthetic networks. The vertical axis is the Area Under the Curve (AUC) for Receiver Operating Characteristics (ROC) analysis, where an AUC = 1 indicates a perfect network recovery and AUC = 0.5 random assignment. Whiskers are related to the 95% confidence interval, green diamonds represent outliers, orange lines represent medians, and boxes are drawn from the first quartile to the third quartile. It is clearly seen that lsAGC outperforms cross-correlation over all tested time-series lengths and noise levels.

the two cohorts in future research. We also find from visual inspection of Fig. 2 that the features extracted by the two methods are likely different, where the mean connectivity matrices for lsAGC appear to be more “sparse” than for cross-correlation. To quantify this qualitative visual impression, we calculated the entropy of the connectivity matrix elements for each of the 59 subjects as a surrogate for matrix “sparseness”. The mean entropy for healthy controls with lsAGC and correlation was 1.66 ± 0.14 and 4.76 ± 0.07 , respectively, and the mean entropy for the ASD patients with lsAGC and correlation was 1.75 ± 0.12 and 4.78 ± 0.07 , respectively. I.e., for both cohorts, the sparseness of lsAGC connectivity matrices appears to be higher than for cross-correlation analysis. We found that this difference between methods, as expressed by the entropy of the connectivity matrix elements, was statistically significant (Mann-Whitney U-test, $p < 10^{-8}$). We conclude that lsAGC may be useful for disease-related classification or regression tasks on clinical fMRI data, because it may extract relevant features potentially not captured by cross-correlation, which is currently used as the mainstay of fMRI connectivity analysis. This hypothesis can be further investigated in future research.

5. CONCLUSIONS

In this work, we have introduced large-scale Augmented Granger Causality (lsAGC) as a method for connectivity analysis in complex systems. The lsAGC algorithm combines dimension reduction with source time-series augmentation and uses multivariate predictive time-series modeling for estimating directed causal relationships among time-series. We quantitatively evaluated the performance of lsAGC on synthetic directional time-series networks with known ground truth. Using simulations for a wide range of time-series lengths and different signal-to-noise ratios, we compared lsAGC with cross-correlation, which is currently used as the clinical standard for fMRI connectivity analysis. We found that lsAGC consistently outperformed cross-correlation at accurately detecting network connections. In addition, we performed a preliminary qualitative analysis of connectivity matrices for fMRI data of Autism Spectrum Disorder (ASD) patients and typical controls, using a subset of the ABIDE II data repository. Our results suggest that lsAGC, by extracting sparse connectivity matrices, may be useful for network analysis in complex systems, and may be applicable to clinical fMRI analysis in future research, such as targeting disease-related classification or regression tasks on clinical data.

ACKNOWLEDGMENTS

This research was funded by Ernest J. Del Monte Institute for Neuroscience Award from the Harry T. Mangurian Jr. Foundation. This work was conducted as a Practice Quality Improvement (PQI) project related to American Board of Radiology (ABR) Maintenance of Certificate (MOC) for Prof. Dr. Axel Wismüller. This work is not being and has not been submitted for publication or presentation elsewhere.

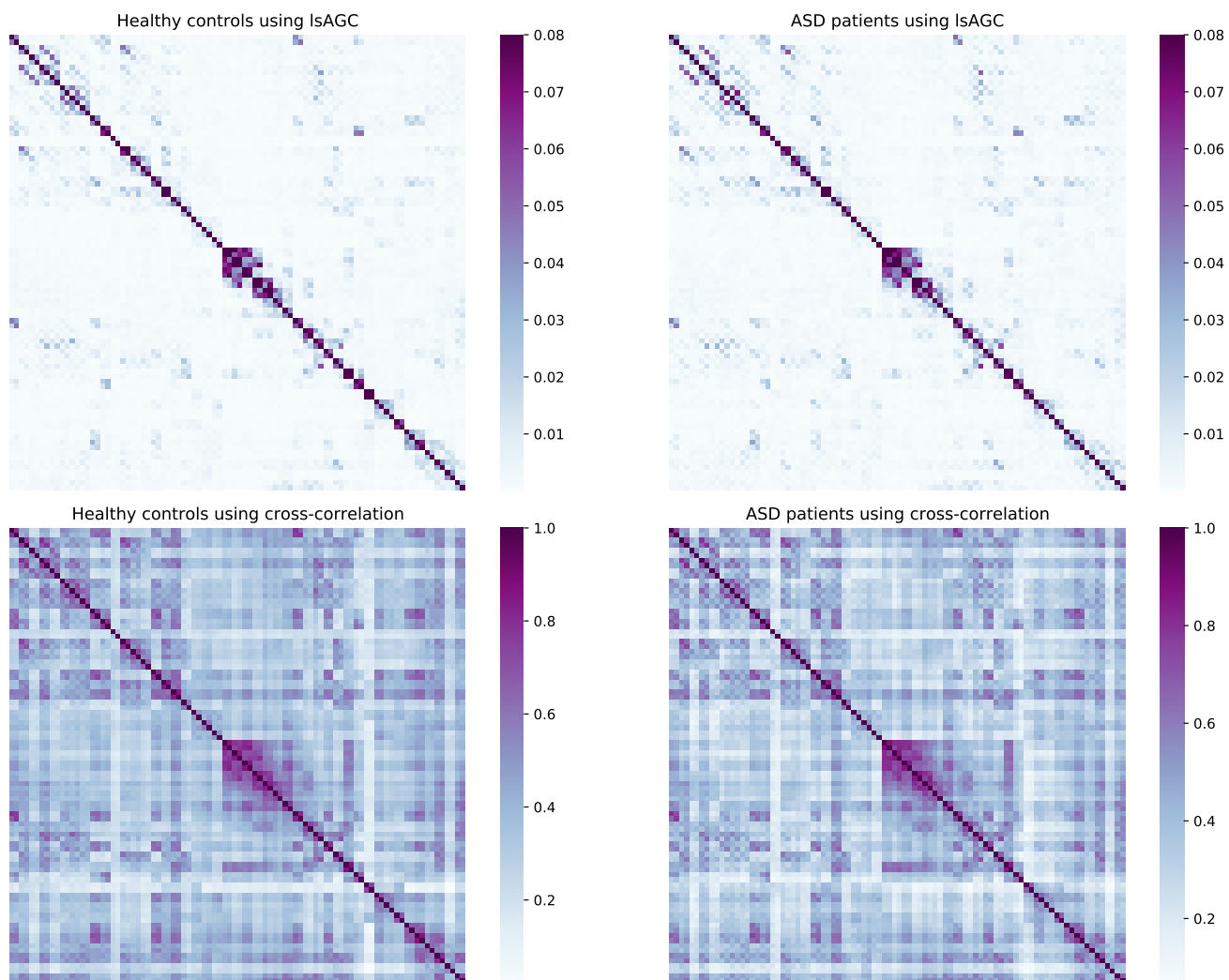


Figure 2. Averaged connectivity matrices: top left: average connectivity matrix of healthy control subjects using lsAGC, top right: average connectivity matrix of ASD patients using lsAGC, bottom left: average connectivity matrix of healthy control subjects using cross-correlation, and bottom right: average connectivity matrix of ASD patients using cross-correlation. Note that the different methods capture different connectivity features, and that there are slight differences of connectivity patterns between healthy subjects and ASD patients. Also, the lsAGC connectivity matrices appear to be significantly “sparser” than cross-correlation matrices. This observation is quantitatively confirmed by calculating the entropy over the matrix elements, as explained in the text.

REFERENCES

- [1] Schreiber, T., “Measuring information transfer,” *Physical review letters* **85**(2), 461 (2000).
- [2] Kraskov, A., Stögbauer, H., and Grassberger, P., “Estimating mutual information,” *Physical review E* **69**(6), 066138 (2004).
- [3] Mozaffari, M. and Yilmaz, Y., “Online multivariate anomaly detection and localization for high-dimensional settings,” *arXiv preprint arXiv:1905.07107* (2019).
- [4] Mozaffari, M. and Yilmaz, Y., “Online anomaly detection in multivariate settings,” in [*2019 IEEE 29th International Workshop on Machine Learning for Signal Processing (MLSP)*], 1–6, IEEE (2019).
- [5] Barnett, L., Barrett, A. B., and Seth, A. K., “Granger causality and transfer entropy are equivalent for Gaussian variables,” *Physical review letters* **103**(23), 238701 (2009).
- [6] Vosoughi, M. A. and Wismüller, A., “Large-scale kernelized Granger causality to infer topology of directed graphs with applications to brain networks,” *arXiv preprint arXiv:2011.08261* (2020).
- [7] Wismüller, A., DSouza, A. M., Abidin, A. Z., and Vosoughi, M. A., “Large-scale nonlinear Granger causality: A data-driven, multivariate approach to recovering directed networks from short time-series data,” *arXiv preprint arXiv:2009.04681* (2020).
- [8] D’Souza, A. M., Abidin, A. Z., Leistritz, L., and Wismüller, A., “Large-scale Granger causality analysis on resting-state functional MRI,” in [*Medical Imaging 2016: Biomedical Applications in Molecular, Structural, and Functional Imaging*], **9788**, 97880L, International Society for Optics and Photonics (2016).
- [9] DSouza, A. M., Abidin, A. Z., Leistritz, L., and Wismüller, A., “Exploring connectivity with large-scale Granger causality on resting-state functional MRI,” *Journal of neuroscience methods* **287**, 68–79 (2017).
- [10] Vosoughi, M. A. and Wismüller, A., “Large-scale extended Granger causality for classification of marijuana users from functional MRI,” *arXiv preprint arXiv:2101.01832* (2021).
- [11] Leinsinger, G., Schlossbauer, T., Scherr, M., Lange, O., Reiser, M., and Wismüller, A., “Cluster analysis of signal-intensity time course in dynamic breast MRI: does unsupervised vector quantization help to evaluate small mammographic lesions?,” *European radiology* **16**(5), 1138–1146 (2006).
- [12] Wismüller, A., Vietze, F., Behrends, J., Meyer-Baese, A., Reiser, M., and Ritter, H., “Fully automated biomedical image segmentation by self-organized model adaptation,” *Neural Networks* **17**(8-9), 1327–1344 (2004).
- [13] Nattkemper, T. W. and Wismüller, A., “Tumor feature visualization with unsupervised learning,” *Medical Image Analysis* **9**(4), 344–351 (2005).

- [14] Bunte, K., Hammer, B., Wismüller, A., and Biehl, M., “Adaptive local dissimilarity measures for discriminative dimension reduction of labeled data,” *Neurocomputing* **73**(7-9), 1074–1092 (2010).
- [15] Wismüller, A., Vietze, F., and Dersch, D. R., “Segmentation with neural networks,” in [*Handbook of medical imaging*], 107–126, Academic Press, Inc. (2000).
- [16] Hoole, P., Wismüller, A., Leinsinger, G., Kroos, C., Geumann, A., and Inoue, M., “Analysis of tongue configuration in multi-speaker, multi-volume MRI data,” (2000).
- [17] Wismüller, A., “Exploratory morphogenesis (XOM): a novel computational framework for self-organization,” *Ph. D. thesis, Technical University of Munich, Department of Electrical and Computer Engineering* (2006).
- [18] Wismüller, A., Dersch, D. R., Lipinski, B., Hahn, K., and Auer, D., “A neural network approach to functional MRI pattern analysis—clustering of time-series by hierarchical vector quantization,” in [*International Conference on Artificial Neural Networks*], 857–862, Springer (1998).
- [19] Wismüller, A., Vietze, F., Dersch, D. R., Behrends, J., Hahn, K., and Ritter, H., “The deformable feature map—a novel neurocomputing algorithm for adaptive plasticity in pattern analysis,” *Neurocomputing* **48**(1-4), 107–139 (2002).
- [20] Behrends, J., Hoole, P., Leinsinger, G. L., Tillmann, H. G., Hahn, K., Reiser, M., and Wismüller, A., “A segmentation and analysis method for MRI data of the human vocal tract,” in [*Bildverarbeitung für die Medizin 2003*], 186–190, Springer (2003).
- [21] Wismüller, A., “Neural network computation in biomedical research: chances for conceptual cross-fertilization,” *Theory in Biosciences* (1997).
- [22] Bunte, K., Hammer, B., Villmann, T., Biehl, M., and Wismüller, A., “Exploratory observation machine (XOM) with Kullback-Leibler divergence for dimensionality reduction and visualization.,” in [*ESANN*], **10**, 87–92 (2010).
- [23] Wismüller, A., Vietze, F., Dersch, D. R., Hahn, K., and Ritter, H., “The deformable feature map—adaptive plasticity for function approximation,” in [*International Conference on Artificial Neural Networks*], 123–128, Springer (1998).
- [24] Wismüller, A., “The exploration machine—a novel method for data visualization,” in [*International Workshop on Self-Organizing Maps*], 344–352, Springer (2009).
- [25] Wismüller, A., “Method, data processing device and computer program product for processing data,” (July 28 2009). US Patent 7,567,889.
- [26] Huber, M. B., Nagarajan, M., Leinsinger, G., Ray, L. A., and Wismüller, A., “Classification of interstitial lung disease patterns with topological texture features,” in [*Medical Imaging 2010: Computer-Aided Diagnosis*], **7624**, 762410, International Society for Optics and Photonics (2010).

- [27] Wismüller, A., “The exploration machine: a novel method for analyzing high-dimensional data in computer-aided diagnosis,” in [*Medical Imaging 2009: Computer-Aided Diagnosis*], **7260**, 72600G, International Society for Optics and Photonics (2009).
- [28] Bunte, K., Hammer, B., Villmann, T., Biehl, M., and Wismüller, A., “Neighbor embedding XOM for dimension reduction and visualization,” *Neurocomputing* **74**(9), 1340–1350 (2011).
- [29] Meyer-Bäse, A., Lange, O., Wismüller, A., and Ritter, H., “Model-free functional MRI analysis using topographic independent component analysis,” *International journal of neural systems* **14**(04), 217–228 (2004).
- [30] Wismüller, A., “A computational framework for nonlinear dimensionality reduction and clustering,” in [*International Workshop on Self-Organizing Maps*], 334–343, Springer (2009).
- [31] Meyer-Base, A., Auer, D., and Wismüller, A., “Topographic independent component analysis for fMRI signal detection,” in [*Proceedings of the International Joint Conference on Neural Networks, 2003.*], **1**, 601–605, IEEE (2003).
- [32] Meyer-Baese, A., Schlossbauer, T., Lange, O., and Wismüller, A., “Small lesions evaluation based on unsupervised cluster analysis of signal-intensity time courses in dynamic breast MRI,” *International journal of biomedical imaging* **2009** (2009).
- [33] Wismüller, A., Lange, O., Auer, D., and Leinsinger, G., “Model-free functional MRI analysis for detecting low-frequency functional connectivity in the human brain,” in [*Medical Imaging 2010: Computer-Aided Diagnosis*], **7624**, 76241M, International Society for Optics and Photonics (2010).
- [34] Meyer-Bäse, A., Saalbach, A., Lange, O., and Wismüller, A., “Unsupervised clustering of fMRI and MRI time series,” *Biomedical Signal Processing and Control* **2**(4), 295–310 (2007).
- [35] Huber, M. B., Nagarajan, M. B., Leinsinger, G., Eibel, R., Ray, L. A., and Wismüller, A., “Performance of topological texture features to classify fibrotic interstitial lung disease patterns,” *Medical Physics* **38**(4), 2035–2044 (2011).
- [36] Wismüller, A., Verleysen, M., Aupetit, M., and Lee, J. A., “Recent advances in nonlinear dimensionality reduction, manifold and topological learning,” in [*ESANN*], (2010).
- [37] Meyer-Baese, A., Lange, O., Wismüller, A., and Hurdal, M. K., “Analysis of dynamic susceptibility contrast MRI time series based on unsupervised clustering methods,” *IEEE Transactions on Information Technology in Biomedicine* **11**(5), 563–573 (2007).
- [38] Wismüller, A., Behrends, J., Hoole, P., Leinsinger, G. L., Reiser, M. F., and Westesson, P.-L., “Human vocal tract analysis by in vivo 3d MRI during phonation: a complete system for imaging, quantitative modeling,

and speech synthesis,” in [*International Conference on Medical Image Computing and Computer-Assisted Intervention*], 306–312, Springer (2008).

- [39] Wismüller, A., “Method and device for representing multichannel image data,” (Nov. 17 2015). US Patent 9,189,846.
- [40] Huber, M. B., Bunte, K., Nagarajan, M. B., Biehl, M., Ray, L. A., and Wismüller, A., “Texture feature ranking with relevance learning to classify interstitial lung disease patterns,” *Artificial intelligence in medicine* **56**(2), 91–97 (2012).
- [41] Wismüller, A., Meyer-Baese, A., Lange, O., Reiser, M. F., and Leinsinger, G., “Cluster analysis of dynamic cerebral contrast-enhanced perfusion MRI time-series,” *IEEE transactions on medical imaging* **25**(1), 62–73 (2005).
- [42] Twellmann, T., Saalbach, A., Muller, C., Nattkemper, T. W., and Wismüller, A., “Detection of suspicious lesions in dynamic contrast enhanced MRI data,” in [*The 26th Annual International Conference of the IEEE Engineering in Medicine and Biology Society*], **1**, 454–457, IEEE (2004).
- [43] Otto, T. D., Meyer-Baese, A., Hurdal, M., Summers, D., Auer, D., and Wismüller, A., “Model-free functional MRI analysis using cluster-based methods,” in [*Intelligent Computing: Theory and Applications*], **5103**, 17–24, International Society for Optics and Photonics (2003).
- [44] Varini, C., Nattkemper, T. W., Degenhard, A., and Wismüller, A., “Breast MRI data analysis by lle,” in [*2004 IEEE International Joint Conference on Neural Networks (IEEE Cat. No. 04CH37541)*], **3**, 2449–2454, IEEE (2004).
- [45] Huber, M. B., Lancianese, S. L., Nagarajan, M. B., Ikpot, I. Z., Lerner, A. L., and Wismüller, A., “Prediction of biomechanical properties of trabecular bone in mr images with geometric features and support vector regression,” *IEEE Transactions on Biomedical Engineering* **58**(6), 1820–1826 (2011).
- [46] Meyer-Base, A., Pilyugin, S. S., and Wismüller, A., “Stability analysis of a self-organizing neural network with feedforward and feedback dynamics,” in [*2004 IEEE International Joint Conference on Neural Networks (IEEE Cat. No. 04CH37541)*], **2**, 1505–1509, IEEE (2004).
- [47] Meyer-Baese, A., Lange, O., Schlossbauer, T., and Wismüller, A., “Computer-aided diagnosis and visualization based on clustering and independent component analysis for breast MRI,” in [*2008 15th IEEE International Conference on Image Processing*], 3000–3003, IEEE (2008).
- [48] Wismüller, A., Meyer-Bäse, A., Lange, O., Schlossbauer, T., Kallergi, M., Reiser, M., and Leinsinger, G., “Segmentation and classification of dynamic breast magnetic resonance image data,” *Journal of Electronic Imaging* **15**(1), 013020 (2006).

- [49] Bhole, C., Pal, C., Rim, D., and Wismüller, A., “3d segmentation of abdominal ct imagery with graphical models, conditional random fields and learning,” *Machine vision and applications* **25**(2), 301–325 (2014).
- [50] Nagarajan, M. B., Coan, P., Huber, M. B., Diemoz, P. C., Glaser, C., and Wismüller, A., “Computer-aided diagnosis in phase contrast imaging x-ray computed tomography for quantitative characterization of ex vivo human patellar cartilage,” *IEEE Transactions on Biomedical Engineering* **60**(10), 2896–2903 (2013).
- [51] Wismüller, A., Meyer-Bäse, A., Lange, O., Auer, D., Reiser, M. F., and Summers, D., “Model-free functional MRI analysis based on unsupervised clustering,” *Journal of Biomedical Informatics* **37**(1), 10–18 (2004).
- [52] Meyer-Baese, A., Wismüller, A., Lange, O., and Leinsinger, G., “Computer-aided diagnosis in breast MRI based on unsupervised clustering techniques,” in [*Intelligent Computing: Theory and Applications II*], **5421**, 29–37, International Society for Optics and Photonics (2004).
- [53] Nagarajan, M. B., Coan, P., Huber, M. B., Diemoz, P. C., Glaser, C., and Wismüller, A., “Computer-aided diagnosis for phase-contrast x-ray computed tomography: quantitative characterization of human patellar cartilage with high-dimensional geometric features,” *Journal of digital imaging* **27**(1), 98–107 (2014).
- [54] Nagarajan, M. B., Huber, M. B., Schlossbauer, T., Leinsinger, G., Krol, A., and Wismüller, A., “Classification of small lesions on dynamic breast MRI: Integrating dimension reduction and out-of-sample extension into cadx methodology,” *Artificial intelligence in medicine* **60**(1), 65–77 (2014).
- [55] Yang, C.-C., Nagarajan, M. B., Huber, M. B., Carballido-Gamio, J., Bauer, J. S., Baum, T. H., Eckstein, F., Lochmüller, E.-M., Majumdar, S., Link, T. M., et al., “Improving bone strength prediction in human proximal femur specimens through geometrical characterization of trabecular bone microarchitecture and support vector regression,” *Journal of electronic imaging* **23**(1), 013013 (2014).
- [56] Wismüller, A., Nagarajan, M. B., Witte, H., Pester, B., and Leistriz, L., “Pair-wise clustering of large scale Granger causality index matrices for revealing communities,” in [*Medical Imaging 2014: Biomedical Applications in Molecular, Structural, and Functional Imaging*], **9038**, 90381R, International Society for Optics and Photonics (2014).
- [57] Wismüller, A., Wang, X., DSouza, A. M., and Nagarajan, M. B., “A framework for exploring non-linear functional connectivity and causality in the human brain: mutual connectivity analysis (mca) of resting-state functional MRI with convergent cross-mapping and non-metric clustering,” *arXiv preprint arXiv:1407.3809* (2014).
- [58] Schmidt, C., Pester, B., Nagarajan, M., Witte, H., Leistriz, L., and Wismüller, A., “Impact of multivariate Granger causality analyses with embedded dimension reduction on network modules,” in [*2014 36th Annual International Conference of the IEEE Engineering in Medicine and Biology Society*], 2797–2800, IEEE (2014).

- [59] Wismüller, A., Abidin, A. Z., D'Souza, A. M., Wang, X., Hobbs, S. K., Leistriz, L., and Nagarajan, M. B., "Nonlinear functional connectivity network recovery in the human brain with mutual connectivity analysis (MCA): convergent cross-mapping and non-metric clustering," in [*Medical Imaging 2015: Biomedical Applications in Molecular, Structural, and Functional Imaging*], **9417**, 94170M, International Society for Optics and Photonics (2015).
- [60] Wismüller, A., Abidin, A. Z., DSouza, A. M., and Nagarajan, M. B., "Mutual connectivity analysis (MCA) for nonlinear functional connectivity network recovery in the human brain using convergent cross-mapping and non-metric clustering," in [*Advances in Self-Organizing Maps and Learning Vector Quantization*], 217–226, Springer (2016).
- [61] Schmidt, C., Pester, B., Schmid-Hertel, N., Witte, H., Wismüller, A., and Leistriz, L., "A multivariate Granger causality concept towards full brain functional connectivity," *PloS one* **11**(4) (2016).
- [62] Abidin, A. Z., Chockanathan, U., DSouza, A. M., Inglese, M., and Wismüller, A., "Using large-scale Granger causality to study changes in brain network properties in the clinically isolated syndrome (CIS) stage of multiple sclerosis," in [*Medical Imaging 2017: Biomedical Applications in Molecular, Structural, and Functional Imaging*], **10137**, 101371B, International Society for Optics and Photonics (2017).
- [63] Chen, L., Wu, Y., DSouza, A. M., Abidin, A. Z., Wismüller, A., and Xu, C., "MRI tumor segmentation with densely connected 3d cnn," in [*Medical Imaging 2018: Image Processing*], **10574**, 105741F, International Society for Optics and Photonics (2018).
- [64] Abidin, A. Z., DSouza, A. M., Nagarajan, M. B., Wang, L., Qiu, X., Schifitto, G., and Wismüller, A., "Alteration of brain network topology in HIV-associated neurocognitive disorder: A novel functional connectivity perspective," *NeuroImage: Clinical* **17**, 768–777 (2018).
- [65] Abidin, A. Z., Deng, B., DSouza, A. M., Nagarajan, M. B., Coan, P., and Wismüller, A., "Deep transfer learning for characterizing chondrocyte patterns in phase contrast x-ray computed tomography images of the human patellar cartilage," *Computers in biology and medicine* **95**, 24–33 (2018).
- [66] DSouza, A. M., Abidin, A. Z., Chockanathan, U., Schifitto, G., and Wismüller, A., "Mutual connectivity analysis of resting-state functional MRI data with local models," *NeuroImage* **178**, 210–223 (2018).
- [67] Chockanathan, U., DSouza, A. M., Abidin, A. Z., Schifitto, G., and Wismüller, A., "Automated diagnosis of HIV-associated neurocognitive disorders using large-scale Granger causality analysis of resting-state functional MRI," *Computers in Biology and Medicine* **106**, 24–30 (2019).
- [68] Wismüller, A. and Vosoughi, M. A., "Classification of schizophrenia from functional MRI using large-scale extended Granger causality," *arXiv preprint* (2021).

- [69] Baccalá, L. A. and Sameshima, K., “Partial directed coherence: a new concept in neural structure determination,” *Biological cybernetics* **84**(6), 463–474 (2001).
- [70] DSouza, A. M., Abidin, A. Z., and Wismüller, A., “Classification of autism spectrum disorder from resting-state fMRI with mutual connectivity analysis,” in [*Medical Imaging 2019: Biomedical Applications in Molecular, Structural, and Functional Imaging*], **10953**, 109531D, International Society for Optics and Photonics (2019).
- [71] First, M., Spitzer, R., Gibbon, M., and Williams, J., “Structured clinical interview for dsm-iv axis i disorders (scid). new york, new york state psychiatric institute,” *Biometrics Research* (1995).
- [72] Whitfield-Gabrieli, S. and Nieto-Castanon, A., “Conn: a functional connectivity toolbox for correlated and anticorrelated brain networks,” *Brain connectivity* **2**(3), 125–141 (2012).
- [73] Wismüller, A., Lange, O., Dersch, D. R., Leinsinger, G. L., Hahn, K., Pütz, B., and Auer, D., “Cluster analysis of biomedical image time-series,” *International Journal of Computer Vision* **46**(2), 103–128 (2002).
- [74] Tzourio-Mazoyer, N., Landeau, B., Papathanassiou, D., Crivello, F., Etard, O., Delcroix, N., Mazoyer, B., and Joliot, M., “Automated anatomical labeling of activations in spm using a macroscopic anatomical parcellation of the mni MRI single-subject brain,” *Neuroimage* **15**(1), 273–289 (2002).